Lipid droplet analysis in caveolin-deficient adipocytes: alterations in surface phospholipid composition and maturation defects[s]

Cédric M. Blouin,* Soazig Le Lay,* Anita Eberl,[†] Harald C. Köfeler,[†] Ida Chiara Guerrera,[§] Christophe Klein,* Xavier Le Liepvre,* Françoise Lasnier,* Olivier Bourron,* Jean-François Gautier,* Pascal Ferré,* Eric Hajduch,* and Isabelle Dugail[1,]*

Centre de Recherche des Cordeliers, INSERM, U872, Université Pierre et Marie Curie - Paris6, and Université Paris Descartes, UMR S 872,* Paris, F-75006 France; Plateau Protéome Necker, PPN, IFR94, Université Paris-Descartes, Faculté de Médecine René Descartes,[†] Paris, F-75015 France; and Center for Medical Research,[§] Medical University, Graz, Austria

Abstract Caveolins form plasmalemnal invaginated caveolae. They also locate around intracellular lipid droplets but their role in this location remains unclear. By studying primary adipocytes that highly express caveolin-1, we characterized the impact of caveolin-1 deficiency on lipid droplet proteome and lipidome. We identified several missing proteins on the lipid droplet surface of caveolin-deficient adipocytes and showed that the caveolin-1 lipid droplet pool is organized as multi-protein complexes containing cavin-1, with similar dynamics as those found in caveolae. On the lipid side, caveolin deficiency did not qualitatively alter neutral lipids in lipid droplet, but significantly reduced the relative abundance of surface phospholipid species: phosphatidylserine and lysophospholipids. Caveolin-deficient adipocytes can form only small lipid droplets, suggesting that the caveolin-lipid droplet pool might be involved in lipid droplet size regulation. Accordingly, we show that caveolin-1 concentration on adipocyte lipid droplets positively correlated with lipid droplet size in obese rodent models and human adipocytes. Moreover, rescue experiments by caveolin- green fluorescent protein in caveolin-deficient cells exposed to fatty acid overload demonstrated that caveolin-coated lipid droplets were able to grow larger than caveolin-devoid lipid droplets.▪ Altogether, these data demonstrate that the lipid droplet-caveolin pool impacts on phospholipid and protein surface composition of lipid droplets and suggest a functional role on lipid droplet expandability.—Blouin, C. M., S. Le Lay, A. Eberl, H. C. Köfeler, I. C. Guerrera, C. Klein, X. Le Liepvre, F. Lasnier, O. Bourron, J-F. Gautier, P. Ferré, E. Hajduch, and I. Dugail. Lipid droplet analysis in caveolin-deficient adipocytes: alterations in surface phospholipid composition and maturation defects. *J. Lipid Res.* 2010. **51:** 945–956.

Supplementary key words obesity • phospholipids • triacylglycerol • lipid storage

The storage of fatty acids as neutral lipids is essential for energy homeostasis. As universal organelles dedicated to this process, lipid droplets can emerge in almost every cell type. Lipid droplets are made of a neutral lipid core, surrounded by a phospholipid monolayer to which surface proteins can associate (1). The most abundant lipid droplet surface proteins defined as the PAT family, consist of the adipocyte specific Perilipin, and the ubiquitous Adipocyte Differentiation-Related Protein (ADRP) and the Tail-Interacting Protein 47 (TIP47) (2), which actively participate in the control of lipid storage and mobilization. Long considered as inert lipid deposits within the cytoplasm, lipid droplets are now recognized as dynamic intracellular organelles, a view that emerged mainly from the larger-than-expected diversity of the lipid droplet proteome that is comprised not only of enzymes of lipid metabolism, but also of proteins involved in intracellular trafficking or signaling (3–8). Nevertheless, most lipid droplet-associated proteins identified by proteomic analysis have not yet been assigned a precise function in the context of lipid storage, and their roles on the lipid droplet surface remain unclear. Consequently, the unexpected

presence of caveolins [primarily known as coating proteins of plasma membrane caveolae (9)] remains poorly understood.

At the plasma membrane, caveolins are involved in multiple cellular functions related to endocytosis, signaling, or lipid trafficking. Adipocytes highly express caveolins, contain numerous plasmalemmal caveolae, and are specialized in the storage of energy in their prominent unilocular lipid droplet. In fat cells, multiple aspects of lipid metabolism linked to plasma membrane function, such as insulin signaling (10) and fatty acid uptake (11), appear to be modulated by caveolins. In agreement, mice with caveolin-1 gene deletion show defective adipose tissue lipid storage and can produce only small adipocytes with lipid droplets of a reduced size (12). Moreover, caveolin-1 was recently identified as a new locus for human congenital lipodystrophy (13), indicating that caveolin-1 is required for appropriate adipose lipid storage in humans.

The direct association of caveolins with the lipid droplet surface has been reported by several groups working on different cultured cell types, including adipocytes (14–19), but no precise attention has so far been given to the function of the lipid droplet caveolin pool. Although it is reasonable to consider that the presence of caveolins on lipid droplets might directly influence organelle function, little experimental evidence supporting this is as yet available. One study reported a role for caveolin in facilitating adipocyte lipolysis and fatty acid mobilization from lipid droplets by hormone sensitive lipase (20). However, blunted lipolysis is hardly compatible with the lean phenotype of caveolin-deficient mice, suggesting that the adipocyte lipid droplet caveolin pool might serve other functions.

In the present study, we wished to examine in detail the role of the adipocyte lipid droplet caveolin pool and its contribution to the function of lipid droplets. To this aim, we applied a set of analytic tools to discern alterations in lipid droplet composition (proteome and lipidome) in caveolin-1 deficient adipocytes. We demonstrated that caveolin-1 regulates the composition of the lipid droplet surface and provides functional support for a role of the caveolin-1 lipid droplet pool in the regulation of lipid droplet expandability.

MATERIALS AND METHODS

Materials

Antibodies used in this study were purchased from the following sources: anti-caveolin-1, anti-caveolin-2, anti-PTRF (BD Biosciences), anti-Glut4 (Cell Signaling), anti-perilipin (Progen), anti GRP78 (Santa Cruz), and anti Golgin58 (Sigma). Antibodies against EHD2, semicarbazide-sensitive amine oxidase (SSAO), Porin, and Na$^+$/K+-ATPase were generously provided by Steve Caplan (University of Nebraska), Marthe Moldes (Paris, France), Daniel Ricquier (Paris, France), and Frederic Jaisser (Paris, France) respectively. Anti-FAS antiserum was described previously (21). HRP secondary antibodies were from Jackson ImmunoResearch Laboratories.

Human adipose tissue

Subcutaneous abdominal adipose tissue was obtained from nondiabetic subjects undergoing abdominal surgery for different medical reasons at the Department of General Surgery at St. Louis Hospital (Paris, France). Samples were collected with the approval of the Saint-Louis Ethics Committee and all subjects gave their written consent. Subjects on endocrine therapy (e.g., steroids, HRT, thyroxine) or antihypertensive therapy and patients with malignant diseases were excluded.

Animal tissues

Animal studies were conducted according to the French guidelines for the care and use of experimental animals. Caveolin-1 null mice were provided by T. Kurzchalia (MPI, Dresden, Germany). Zucker obese (fa/fa) rats and their lean littermates (fa/+) were obtained from Charles River Laboratories (France). All the experiments were performed on adipocytes isolated from epididymal or subcutaneous fat pads as mentioned.

Isolation of primary adipocytes and fat cell size determination

Adipocytes were isolated by collagenase digestion of fat pads by the method of Rodbell (22). Microscopic images of isolated adipocyte suspensions were collected (at least 200 individual cells corresponding to four different observation fields) and served to estimate mean diameter of adipocytes or isolated lipid droplets using an image analysis software (Claravision).

Cell culture

3T3-L1 cells (kind gift of Dr J. Pairault, Paris, France) were maintained in high-glucose DMEM supplemented with 10% newborn calf serum. Adipocyte differentiation was induced by adding IBMX (100 µM), dexamethasone (0.25 µM), and insulin (1 µg/µl) for 2 days, and cells were then cultured in medium with 10% fetal calf serum and insulin alone for differentiation. Human fibroblasts deficient for caveolin-1 were kindly provided by J. Magré (INSERM, France) and cultured in DMEM/HAMF12 (v/v) supplemented with 10% fetal calf serum.

Preparation of whole cell lysates

Adipocytes were lysed as described previously (23), Whole cell lysates were centrifuged (15,000 g, 4°C for 10 min) and stored at −80°C.

Isolation of lipid droplets

Lipid droplets were isolated as described previously (19). Briefly, adipocytes were washed twice with PBS and resuspended in 3 ml of disruption buffer [25 mM Tris-HCl, 100 mM KCl, 1 mM EDTA, 5 mM EGTA, pH 7.4, 'Complete' protease inhibitor cocktail (Roche Diagnostics, GmBH, Product number 11836145001)]. Cells were disrupted by nitrogen cavitation at 800 psi for 10 min at 10°C. The lysate was collected and mixed with an equal volume of disruption buffer containing 1.08 M sucrose. It was then sequentially overlaid with 2 ml each of 270 mM sucrose buffer, 135 mM sucrose buffer, and Tris/EDTA/EGTA buffer (25 mM Tris-HCl, 1 mM EDTA, 1 mM EGTA, pH 7.4). Following centrifugation at 150,000 g for 60 min, fractions were collected from the top of the gradient.

Assessment of caveolar membrane contamination of lipid droplet fractions

The protocol described in previous studies (24) to isolate detergent-resistant membrane fractions was applied directly to total membranes or isolated lipid droplet fractions isolated as described above.

Immunoblotting

Samples were subjected to SDS/PAGE on 10, 12, or 14% polyacrylamide gels and were transferred onto nitrocellulose membranes (Amersham Biosciences, NJ), blocked for 2 h at room temperature in 5% (w/v) skimmed milk/TBS (50 mM Tris-HCl pH 7.6, 150 mM NaCl) supplemented with 0.1% (v/v) Tween-20) and probed with various antibodies. Nitrocellulose membranes were washed three times in TBS/0.1% (v/v) Tween-20 for 5 min prior to incubation with secondary peroxidase IgGs. Protein signals were visualized using enhanced chemiluminescence (Pierce-Perbio Biotechnology, Germany) by exposure to Kodak autoradiographic film.

Determination of protein concentration

Protein concentrations were determined by the Biorad protein assay kit using BSA as standard.

In-gel tryptic digestion

After silver staining following the method of Shevchenko (25), protein bands were excised from 1-dimensional SDS-PAGE, transferred into a tube containing 1% acetic acid in water, and destained with the Invitrogen silver staining kit following the manufacturer's instructions. Gel pieces were washed twice in water, and in 25 mM ammonium bicarbonate in 50% acetonitrile (ACN), and were finally dehydrated with 100% ACN. Dried gel was placed at 56°C for 1 h in a reducing solution containing 10 mM DTT and 12.5 mM ammonium bicarbonate for cysteine reduction. The supernatant was removed and alkylation of the cysteines was achieved by incubation for 45 min in the dark with 55 mM iodoacetamide in 25 mM ammonium bicarbonate buffer. Gel pieces were washed with 25 mM ammonium bicarbonate in 50% ACN and subsequently dehydrated with 100% ACN. Dried gel pieces were hydrated for 30 min on ice with a solution of 25 mM ammonium bicarbonate and 5 mM $CaCl_2$ solution containing the trypsin (12 ng/µl). After overnight digestion at 37°C with trypsin, peptides were extracted by successive incubation of the gel with 1% trifluoroacetic acid (TFA) in 50% ACN and with pure ACN.

MALDI-MS analysis

Saturated alpha-cyano-4-hydroxycinnamic acid (α-CHCA) matrix was prepared by incubating about 10 mg of matrix with 100 µl of 0.1% TFA in 50% ACN. The mixture was sonified for 5 min, centrifuged for 5 min at 14,000 rpm and diluted 1:3 in 0.1% TFA in 50% ACN. The sample (0.5µl) was spotted on a steel MALDI target plate, 0.5 µl of freshly made α-CHCA matrix was added, and the mixture was left to dry at room temperature. Peptides were analyzed by MALDI-time of flight (TOF) MS using an Autoflex instrument (Bruker Daltonics). Protein identification was performed by Mass Finger Printing using an in-house Mascot 2.2 engine (26) and the protein database used was SWISSPROT in the Mus musculus species.

Nanochromatography

Tryptic digest of protein mixtures were acidified with formic acid (1% final concentration) and separated with an Ultimate3000 (Dionex). Briefly, the sample was injected and trapped using solvent A (0.1% TFA) at a 30 µl/min loading flow for 3 min in a C18 trap column (Dionex). The peptides were then eluted (300nL/min) into the analytical column (C18pepmap100 3 µlm, 15cm length, 75 µm i.d., 100A) in 7% solvent B (80% ACN, 20% solvent A). The gradient used was set to reach 60% of solvent B in 38 min. Fractions were spotted on-line on a MALDI target using a Probot (Dionex) fraction collector. Fractions were mixed 1:9 with 2 mg/ml of α-CHCA (Laser Biolabs) in 70% ACN

(Carlo Erba) 0.1% TFA (Pierce) prior to spotting. A total of 190 fractions were collected and analyzed using a 4800 MALDI TOF TOF analyzer (ABI).

MALDI TOF TOF MS/MS analysis

Spectra acquisition and processing was performed in positive reflection mode at fixed LASER fluency with low mass gate and delayed extraction. For each fraction, steps of 50 MS spectra in the range of 900 to 7000Da were acquired at a 200Hz LASER shot frequency for a total of 3,000 spectra per sample. For each MS spectrum, the eight most abundant peaks were selected for fragmentation. Selection of parent candidate ions was made according to mass range, signal intensity, s/n ratio, and absence of neighboring masses in the MS spectrum. Six thousand MS/MS spectra were summed by increments of 75. Generated and concatenated MS/MS peaklists were subsequently submitted to an in-house mascot search engine (Matrix Science). SwissProt database was used in the Mus musculus species. A filter was applied to the search in order to reduce false positives and matching redundancies of the same peptide in several hits. All matches above 5% risks of random matching were eliminated ($P < 0.05$).

FRAP analysis

Fluorescence recovery after photobleaching (FRAP) experiments were done on a Zeiss LSM510 confocal laser scanning microscope. 3T3-L1 adipocytes were transfected as described previously (27) and plated on 30 mm diameter coverslips and inserted in a mini-poc (Pe-Con) chamber equiped with a heating insert and an incubator both maintained at 37°C. Experiments were made with a Zeiss C-apochromat ×63, NA 1.3 objective. Bleaching and image acquisition were done using the 488 nm line of an argon ion laser (25mW) set to full power. Image acquisition was done with Acousto-Optic Tunable Filters transmission set to 1% while it was set to 100% for bleaching. A circular region of 3µm in diameter (25 pixels) was scanned 10 times for bleaching. Five prebleach and 195 images were recorded to monitor the fluorescence recovery at a frame rate of 0.660 s by frame. Time series were then analyzed with ImageJ software. Data from at least nine fields were averaged, normalized, and the degree of fluorescent recovery determined.

Lipid extraction

Isolated lipid droplets (from ∼0.5ml packed cell volume) were used for lipid extraction according to (28). Prior to extraction, an internal standard mixture containing 5 µM each of 51:0 triacylglycerol (TAG), 24:0 diacylglycerol (DAG), 17:0 cholesterol ester (CE), 24:0 phosphatidylcholine (PC), 24:0 phosphatidylserine (PS), and 24:0 phosphatidylethanalomine (PE) was added. Extracts were dried under nitrogen, reconstituted in ACN/2-propanol 5:2, 1% ammonia acetate, 0.1% formic acid. Chromatography was done by an Accela HPLC (Thermo Scientific, San Jose, CA) equipped with a Hypersil GOLD C18 (100 × 1 mm, 1.9µm) column. Solvent A was water with 1% ammonia acetate and 0.1% formic acid, and solvent B was ACN/2-propanol 5:2 with 1% ammonia acetate and 0.1% formic acid. The gradient ran from 35% to 70% B in 4 min, then to 100% B in another 16 min where it was held for 10 min. The flow rate was 250 µl/min.

Lipid analysis by mass spectrometry

Data acquisition was done on a LTQ-FT (Thermo Scientific, San Jose, CA) by FT-MS full scan at a resolution of 100 k and < 2 ppm mass accuracy with external calibration. The spray voltage was set to 5000 V, capillary voltage to 35 V, and the tube lens was at 120 V. Capillary temperature was at 250° C. Peak areas were calculated by QuanBrowser for all lipid species, identified

previously by exact mass (<2 ppm) and retention time. The calculated peak areas for each species were expressed as % of internal standard in the respective lipid class.

Statistical analysis

Statistical analyses were carried out using Student's *t*-test or one-way ANOVA. Differences were considered statistically significant at *p* values < 0.05 and shown by an asterisk in Figs. 4–6.

RESULTS

Biochemical characterization of lipid droplets isolated from primary adipocytes

A standard procedure for lipid droplet isolation, previously used to define lipid droplet proteome, consists of cell disruption by nitrogen cavitation followed by lipid droplet purification on sucrose gradient (5–7). As a first step, we ensured that this process was applicable to primary mouse adipocytes, in which lipid droplet size range exceeds by at least one order of magnitude that found in all other cell types. We observed that the size distribution of the lipid droplet population obtained after cell disruption closely matched that of freshly isolated fat cells (**Fig.**

1A), indicating that no major structural rearrangements of large lipid droplets, such as uncontrolled fusion or fission events, occurred during isolation. Having established that lipid droplets could be recovered without modifying their size range, we confirmed that required purity standards were fulfilled. We analyzed the fractions obtained by sucrose gradient for presence of several subcellular compartment markers to assess potential contaminations of the lipid droplet fraction (Fig. 1B). As expected, lipid droplets, characterized by high triglyceride content and specific presence of the lipid droplet marker perilipin, were segregated at the top of the gradient, largely in fraction 1. Undetectable contamination with plasma membrane, mitochondria, Golgi, or internal recycling vesicles was indicated by the absence of the corresponding markers in fraction 1. Weak signals for the cytosolic FAS and GRP78, an endoplasmic reticulum resident protein were detected, indicating minor presence of both cytoplasmic or endoplasmic reticulum-associated proteins. Noteworthy, two caveolin isoforms (caveolin-1 and caveolin-2) clearly distributed in the top and the bottom fractions (Fig. 1B, fractions 1 and 7 respectively), which likely represent isolated lipid droplets well separated from caveolin-
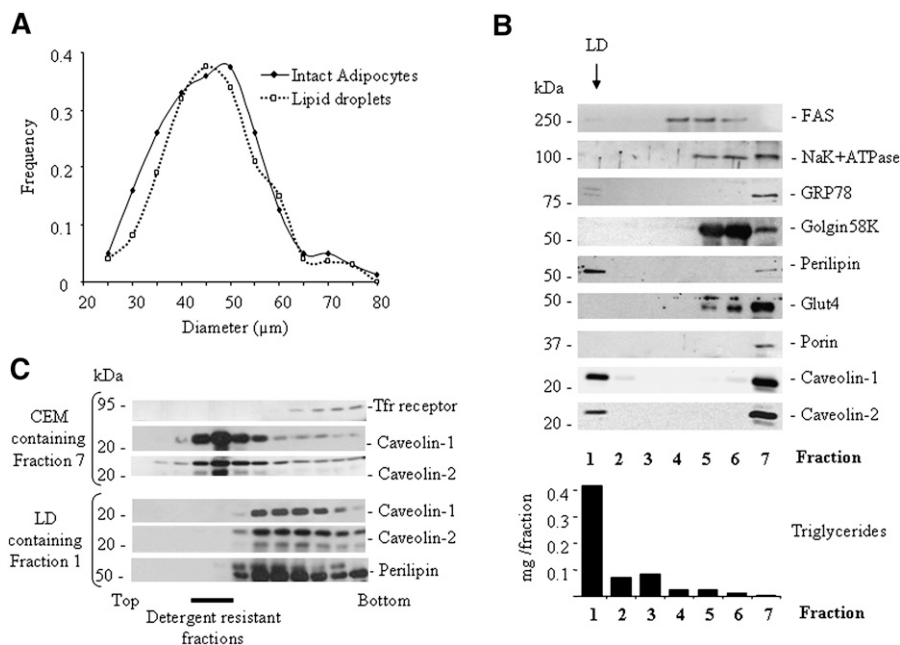

Fig. 1. Purity of lipid droplets isolated from mouse adipocytes. A: Size distribution of a freshly isolated primary adipocyte population (plain lines) from 3-month-old wild-type mice and the corresponding lipid droplets obtained after cell disruption (dotted lines). Due to individual differences in fat cell size distribution within individual mice (range 39.97–59.55 μm), a typical experiment representative of five is presented. B: Purification of lipid droplets by sucrose gradient centrifugation. Following cell disruption by nitrogen cavitation, cell material was submitted to sucrose gradient from which seven fractions were collected from top to bottom of the tube. Each fraction was analyzed by SDS-PAGE. Equal volumes were loaded in each lane for Western blotting with the indicated antibodies. Note that lipid droplets are recovered in fraction 1 with a high triglyceride content (measured with a commercial kit) and the presence of perilipin. Fraction 7 contains caveolin-enriched membranes (CEM). C: Absence of membrane caveolar contamination in lipid droplet fractions. Both fraction 7 (in B) and fraction 1 (in B) were exposed to 1% Triton X-100 at 4°C and centrifuged on a sucrose gradient designed to separate detergent resistant membranes (recovered in fractions 3 to 6). Equal volumes from each fraction were loaded in each lane. Note that no caveolin-1 or -2 signal from lipid droplet fractions be could be detected as detergent resistant, demonstrating the absence of caveolar membrane contamination.

enriched membranes (CEMs). Because we wanted to study the lipid droplet caveolin pool, it was crucial to be certain that lipid droplets could be isolated free of caveolar membrane contaminations. We reasoned that the distinctive property of lipid raft microdomains to resist detergent solubilization could be used to detect the presence of caveolar membranes possibly contaminating the lipid droplet fraction. Lipid droplet-containing fraction 1 and CEM-containing fraction 7 were submitted to Triton X-100 extraction, and the presence of caveolin-1-positive detergent resistant material was tested on a classical discontinuous density gradient (24). From the lipid droplet-containing fraction 1, no caveolin could be detected as detergent resistant, in contrast with what was observed in CEM-containing fraction 7 (Fig. 1C). This clearly indicates that the isolation procedure produces pure lipid droplet fractions, free from caveolar membrane contamination.

Structural organization of the caveolin lipid droplet pool

As a first step to elucidate the role played by the caveolin lipid droplet pool, we established a differential proteomic screening that would reveal changes in adipocyte lipid droplet composition brought about by the presence of caveolins. We compared protein electrophoretic profiles of

lipid droplets in control or caveolin-1 deficient adipocytes obtained from caveolin-1 null mice. SDS-PAGE analysis revealed several bands missing in caveolin-deficient lipid droplets, whereas no additional bands could be clearly identified (**Fig. 2A**). Bands with differential electrophoretic patterns were excised from the gel and the corresponding proteins identified by mass spectrometry by Mascott software (supplementary Table I). When possible, the absence of the identified protein from caveolin lipid droplets was retrospectively confirmed by Western blotting (Fig. 2B). Most proteins found absent in lipid droplet fractions from caveolin-1 null mice had already been found on lipid droplets in previous reports (**Table 1**). Interestingly, among caveolin-dependent lipid droplet-associated proteins we found seven proteins that were known to participate or interact with plasmalemnal caveolae structures. As a salient example, we identified PTRF/cavin, which was recently reported to physically associate and functionally cooperate with caveolin-1 in the formation and stabilization of membrane caveolae (29, 30). In addition, EHD2, a GTPase involved in membrane remodeling previously found in adipocyte caveolar fractions (3), as well as several cytoskeleton-related proteins (two Actin isotypes and an actin-binding mechano-chemical protein, Myosin-1) previ-
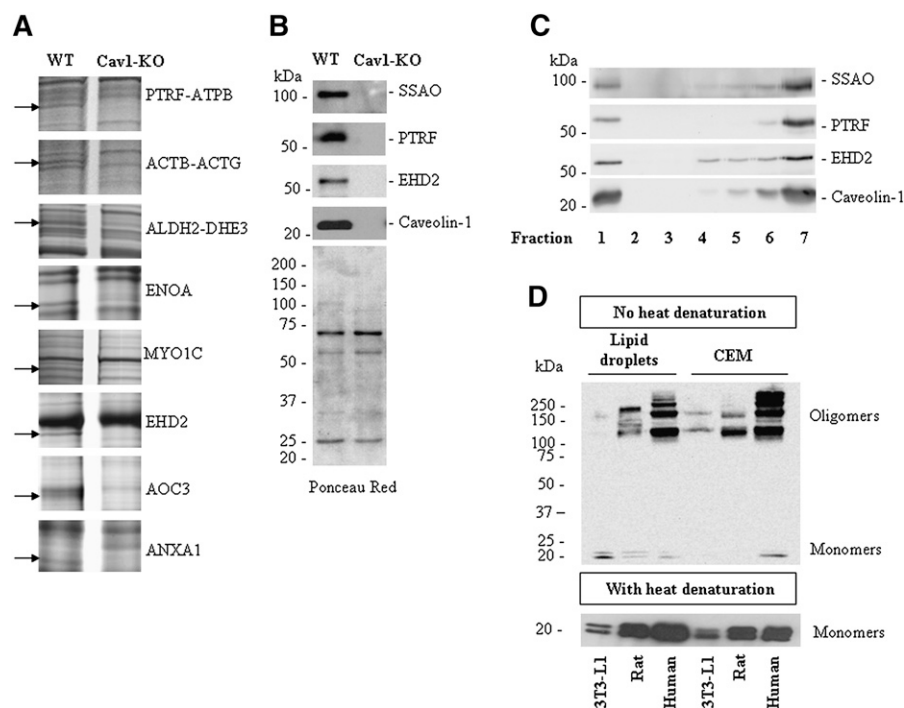

Fig. 2. Caveolin-1 dependent proteome of murine adipocyte lipid droplets. A: Identification of caveolin-dependent lipid droplet associated proteins. Representative SDS-PAGE electrophoretic profiles of isolated adipocyte lipid droplets obtained from control (WT) and caveolin-1 null mice. Gel portions are shown where differential band pattern was observed. Swiss Prot IDs of protein(s) identified in each band are indicated on the right (see also supplementary Table I for Mascott scores). B: Confirmation of the absence of PTRF, SSAO, and EHD2 on lipid droplets from caveolin-1 null mice. Equal protein loading was checked by Ponceau red. C: Confirmation of the presence of PTRF, SSAO, and EHD2 on lipid droplets. Adipocytes were fractionated on sucrose gradients as in Fig. 1B, lipid droplet correspond to fraction 1. D: Oligomeric organization of adipocyte lipid droplet caveolin-1. Electrophoretic profiles of caveolin-1 in total membrane fractions or lipid droplets. Before loading onto the gel, samples were boiled for 5 min for denaturation (lower panel) or incubated at 25°C (no heat denaturation, upper panel). Samples from 3T3-L1, rat, and human adipocytes were resolved and immunoblotted with caveolin-1 antibody.

SwissProt ID	Protein name	Previously found on lipid droplets	Previously found in caveolae
PTRF_MOUSE	Polymerase I and transcript release factor	Bartz et al. 2007 Brasaemle et al. 2004	Aboulaich et al. 2004 Hill et al. 2008 Liu et al. 2008
EHD2_MOUSE	EH domain-containing protein 2	Brasaemle et al. 2004	Aboulaich et al. 2004
MYO1C_MOUSE	Myosin-Ic (Myosin I β) (MMIb)	Bartz et al. 2007	Aboulaich et al. 2004
ACTB_MOUSE	Actin, cytoplasmic 1 (Beta-actin)	Bartz et al. 2007	Aboulaich et al. 2004
ACTG_MOUSE	Actin, cytoplasmic 2 (Gamma-actin)	no	Halayko et al. 2005
ATPB_MOUSE	ATP synthase subunit β, mitochondrial precursor	Brasaemle et al. 2004 Cermelli et al. 2006	Wang et al. 2006
AOC3_MOUSE	Membrane copper amine oxidase (Semicarbazide-sensitive amine oxidase) (SSAO) (Vascular adhesion protein 1) (VAP-1)	no	Souto et al. 2003
ALDH2_MOUSE	Aldehyde dehydrogenase, mitochondrial precursor (ALDH class 2) (AHD-M1) (ALDHI) (ALDH-E2)	Liu et al. 2004	no
ENOA_MOUSE	Alpha-enolase (2-phospho-D-glycerate hydro-lyase) (Non-neural enolase) (NNE) (Enolase 1)	Bartz et al. 2007	no
ANXA1_MOUSE	Annexin A1 (Annexin-1) (Annexin I) (Lipocortin I) (Calpactin II) (Chromobindin-9) (p35) (Phospholipase 2 inhibitory protein)	no	no
DHE3_MOUSE	Glutamate dehydrogenase 1, mitochondrial precursor (GDH)	no	no

This list was established on the basis of identification of the protein in replicated MS analyses from two independent preparations obtained from pooled adipose tissues of 5 to 10 individual mice. Differential electrophoretic pattern was looked at when consistently present in the two independent preparations, and persistent upon overloading of the gels with increasing amounts of LD proteins. Details for statistical significance of protein identification are provided in supplemental Table I.

ously shown to decorate the striped coat of caveolae (31), were found. Furthermore, SSAO, an abundant adipocyte protein located in caveolae was identified on lipid droplets for the first time, and its localization was confirmed in Western blots (Fig. 2C). Because caveolin-deficient lipid droplets are small we wanted to exclude the possibility that proteins could be missing on lipid droplets due to little maturation of the lipid storage organelle unrelated to caveolin deficiency. We isolated lipid droplets from terminally differentiated 3T3-L1 adipocytes to which caveolin can bind (14), despite a small size (average diameter 5–7 microns). We found that in addition to caveolin-1, PTRF, EHD2, and SSAO could also associate with small lipid droplets as demonstrated by Western blotting (data not shown). Thus, they defined a subset of proteins that associate to lipid droplets in a caveolin-dependent manner. The coordinated presence of caveolin-1, cavin-1, and several other caveolar proteins at the lipid droplet site suggests that lipid droplet caveolin is present as a multi-protein complex with similar composition to those formed on caveolae. These data indicate that despite different contexts between lipid droplets and caveolae, (membrane bilayer or monolayer) some resemblance still exists with regard to caveolin organization in the two locations.

To confirm structural similarities between the lipid droplet caveolin pool and plasmalemnal caveolae, we further examined caveolin-1 molecular organization within the two compartments. It is well established that caveolins in caveolae are organized as SDS-resistant, heat-sensitive, highly oligomeric structures that can be visualized on SDS-PAGE as high molecular weight bands provided no heat denaturation of samples was performed before loading onto the gel (32). Accordingly, total membrane preparations from 3T3-L1 cells and from rat and human adipocytes showed abundant high molecular weight caveolin-1 immunoreactive bands (above 150 kDa) indicative of the presence of caveolin oligomers and very low signal, at 20 kDa, the caveolin monomer molecular weight (Fig. 2D). Similar to membrane fractions, lipid droplets also revealed the presence of high molecular weight organized caveolin-1 oligomers, most abundant in rat and human adipocytes (Fig. 2D).

Caveolin dynamics within plasma membrane is another well-known unique feature of cell surface caveolin. Indeed, caveolin oligomers in caveolae have been shown to form highly immobile domains with reduced lateral diffusion (33). To test whether lipid droplet-associated caveolins have similar dynamic properties, we performed FRAP analysis in transfected 3T3L1 adipocytes using a Cav1-green fluorescent protein (GFP) construct which induces the expression of full length caveolin-1 followed by a C-terminally fused green fluorescent protein. We recently reported that in 3T3-L1 adipocytes, caveolin-1 was mainly distributed at the cell surface at early stages of adipocyte differentiation, and became associated to lipid droplets in terminally differentiated mature fat cells (14). Thus, 3T3-L1 adipocytes expressing Cav1-GFP were studied at early and later stages of adipocyte differentiation corresponding to cell surface (**Fig. 3A**) and lipid droplet association (Fig. 3B) of caveolin-1. To study caveolin-1 lateral mobility, fluorescence recovery after bleaching was monitored for a 120 s time period as previously described (33), a scheme that differs from that used by Pol et al. (34), in which longer times for fluorescence recovery (up to 90 min) were necessary to demonstrate the trafficking of caveolin between lipid bodies and the cell surface. Consistent with the study of Pol et al. (33), our FRAP analysis indicated that Cav1-GFP mobility on the cell surface was extremely low, with a mobile fraction of 16.4% (Fig. 3A).
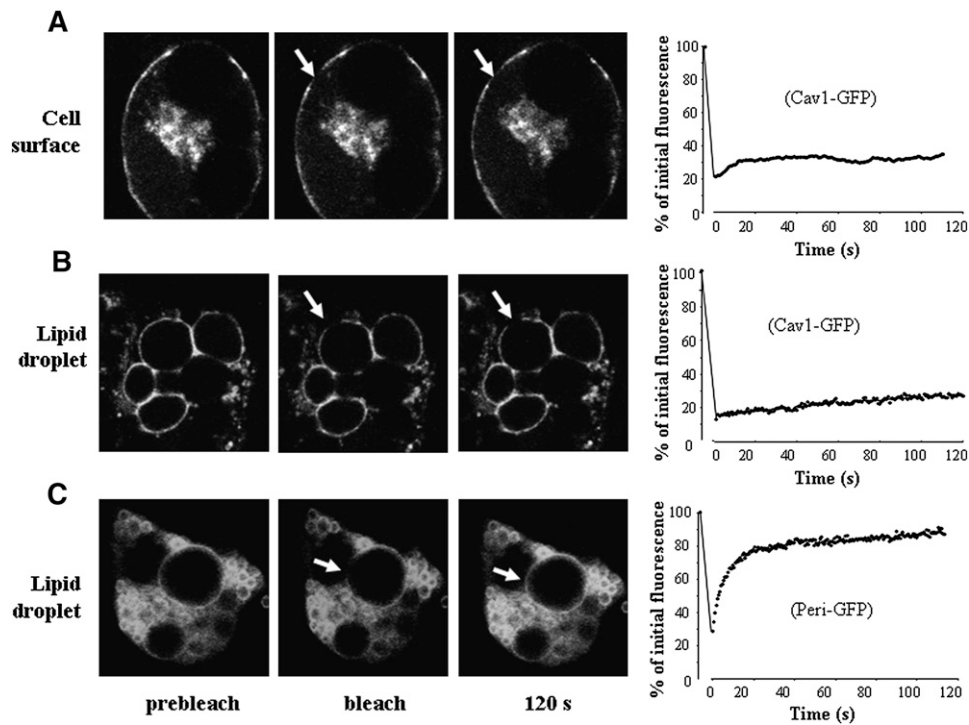
Fig. 3. FRAP analysis of caveolin mobility on lipid droplets. Differentiated 3T3-L1 adipocytes were transiently transfected with caveolin-1-GFP (Cav1-GFP, A and B) or perilipin-GFP (Peri-GFP, C). In each panel, three images show examples of fluorescence distribution before bleaching, immediately after bleaching, and after 120 s. The bleached area (3 µm diameter, 25 pixels) is shown by an arrow. Graphs on the right show mean fluorescence in the bleached area after normalization. At least nine independent FRAP experiments per group were plotted and fitted from a one-phase exponential association. In A and C, cells were studied at an early stage (4–6 days after the induction of differentiation) when caveolin distributes at the cell surface. In B, cells were imaged at a later stage (8–10 days after the induction of differentiation) to visualize lipid droplet caveolin.

On lipid droplets, the mobility of Cav1-GFP was also very limited, and the majority of the Cav1 fusion remained as an immobile pool (Fig. 3B). Such a low mobility at the lipid droplet surface was a unique property of caveolins and was not shared by other lipid droplet-associated proteins. Using the transfection of a perilipin-GFP construct, we observed that perilipin mobility on lipid droplets differed strikingly from that of caveolin-1 (Fig. 3C), as most perilipin at the lipid droplet surface distributed in the mobile fraction (75%) with a half-life in fluorescence recovery of 6.07 s. Thus, caveolin-1 dynamics at the lipid droplet site present properties that strikingly contrast with another lipid droplet protein, and appears to be mostly related to caveolin-1 behavior at the cell surface. Altogether, these data on the organization and dynamics of the lipid droplet caveolin pool point out for the first time a close resemblance with caveolar structures. A striking difference, however, is that invagination of the lipid droplet surface has never been reported to date, likely due to the presence of a neutral lipid core inside the lipid droplet.

Caveolin-1 impacts on phospholipid composition of the lipid droplet surface

In a previous report, we had observed that caveolin-deficient lipid droplets had decreased free cholesterol contents (19). To further characterize potential changes in lipid composition driven by caveolin-1 deficiency on lipid droplets,

we conducted a complete analysis of neutral lipids and surface phospholipids by mass spectrometry, and compared the relative composition of isolated lipid droplets between wild-type and caveolin-1 null mouse adipocytes. Importantly, lipid droplets from Cav-1-null adipocytes are significantly smaller than those from wild-type adipocytes, indicating that they contain less TAG, the major component in the adipocyte lipid droplet core. However, after normalization to lipid droplet protein content, we detected no changes in the relative amounts of TAGs or DAGs between wild-type and caveolin-1 deficient lipid droplets (**Fig. 4B**). Furthermore, among the more than 50 individual TAG species found, none were affected by caveolin deficiency (supplementary Fig. I). Furthermore, PC, SM, PE, and plasmalogens were not significantly affected by caveolin-1 deficiency. In contrast, the relative abundance of phosphatidylserine (PS), and lysophospholipids (mostly found as PC-derived compounds) was significantly reduced in caveolin-1-deficient lipid droplets (Fig. 4C). Closer examination of the molecular profile of lipid droplet-associated phospholipids revealed only minor changes in PC composition between controls and caveolin-deficient lipid droplets (supplementary Fig. I). Within PE species, a trend toward higher proportions of species with 38-carbons chain lengths at the expense of longer ones (40 carbons) was found in lipid droplets lacking caveolin (**Fig. 5A**). Likewise, shifted acyl chain length was also observed for PS (Fig. 5B)
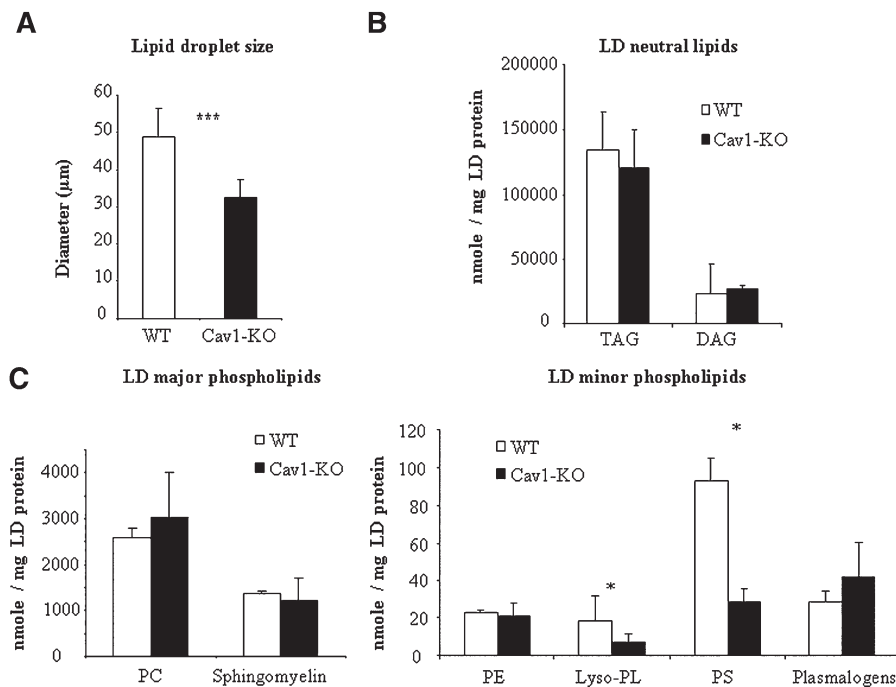
Fig. 4. Comparative lipid analysis in controls and caveolin-deficient lipid droplets. A: Lipid droplet size in controls and caveolin-1 null mice adipocytes. The size of 200 individual lipid droplets was measured in each preparation and the mean lipid droplet diameter ± SEM was calculated. Significant differences (*** $P <$ 0.001) were assessed by paired Student's *t*-test. B and C: Relative abundance of lipid classes in isolated lipid droplets (LD) from wild-type (WT, white bars) or caveolin-1 null (Cav1-KO, black bars) mice. Data are presented as means ± SEM, n = 5. * indicates a significant difference by paired Student's *t*-test, $P < 0.05$.

in which the relative abundance of 36 carbon chains was significantly increased in caveolin-deficient lipid droplets, with a corresponding 2-fold decrease in the major 40 carbon PS species. Sphingomyelin lipid species were similarly affected with shorter chain species 20-22 carbons (including the major 22 carbon SMs) enriched in caveolin-1 null lipid droplets, at the expense of longer 24 SM species (Fig. 5C). Altogether, these data demonstrate that absence of caveolin-1 on lipid droplets affects the lipid droplet surface with regard to phospholipid and protein composition. To approach the functional consequences of these changes, we next examined if the lipid droplet caveolin pool could influence lipid filling and size changes.

The size of lipid droplets is a major determinant of caveolin-1 association

We thus examined whether the lipid droplet caveolin-1 pool could be modulated in animal models of obesity in which a sustained disequilibrium in energy balance induced adipocyte lipid droplet size enlargement (35). We isolated primary adipocytes from adipose tissue of lean (fa/+) or obese (fa/fa) fatty Zucker rats and separated lipid droplets from the bulk of total membranes. In these experiments, the absence of caveolar contamination in lipid droplet fraction was checked again to ascertain that lipid droplet recovery was not altered in obese adipocytes (data not shown). We observed that total caveolin-1 expression in whole cell lysates was not affected by obesity (**Fig. 6A**). However, a 4-fold enrichment in caveolin-1 was found in lipid droplet fractions from

obese compared with lean rats, contrasting with an unaffected perilipin signal (Fig. 6A). Similar results were obtained in subcutaneous and peri-epidydimal fats, indicating that caveolin enrichment of lipid droplets was present in all adipose localizations (data not shown). These data point out that large lipid droplets engorged with triglycerides are specifically enriched with caveolin-1 and suggest a connection between lipid droplet size and caveolin association.

To further explore the relationship between fat cell size variation and caveolin association, we used adipose tissue samples collected from healthy human subjects in which individual variations in adiposity and mean fat cell sizes are commonly found. Indeed, in six subjects within a body mass index range of 24 to 36 (supplementary Table II), mean fat cell diameters varied between subjects from 90 to 120 μm. We observed that, despite comparable total adipocyte caveolin-1 expression between subjects (data not shown), caveolin-1 concentration on lipid droplets was positively correlated ($P < 0.05$) with fat cell size (Fig. 6B). This noticeably differed from perilipin concentration that remained constant in lipid droplets of different sizes. Collectively, these data indicate a new link between lipid droplet caveolin-1 pool and lipid droplet size, and suggest that adipocyte lipid droplet expansion might be specifically linked to caveolin-1 enrichment.

To directly demonstrate that the pool of lipid droplet caveolin could favor size enlargement, we used fibroblasts lacking endogenous caveolin-1 and examined the size of lipid droplets that were formed in the absence of caveo-
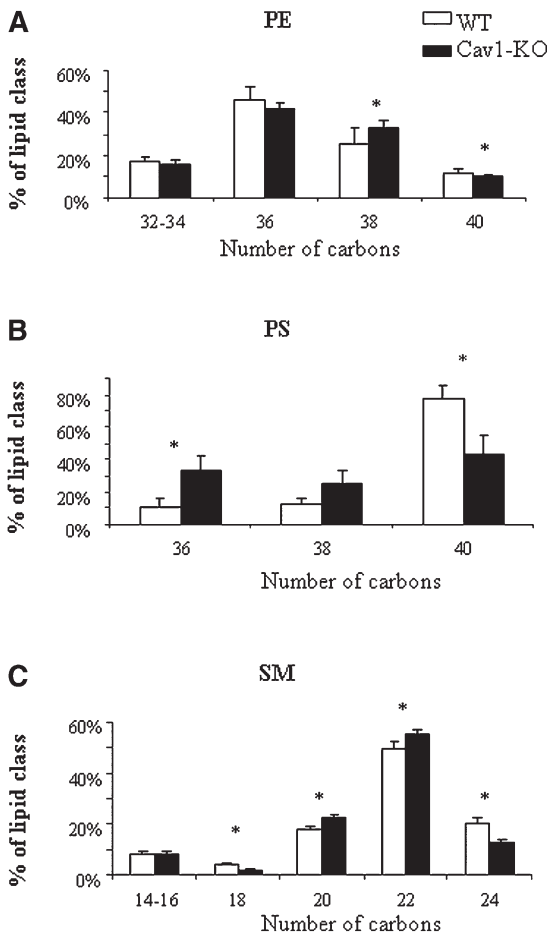
Fig. 5. Alterations in individual phospholipid species in caveolin-deficient lipid droplets. A: Phosphatidylethanolamine (PE). B: Phosphatidylserine (PS). C: Sphingomyelin (SM). Relative levels of individual lipid species sorted according to acyl chain lengths in isolated lipid droplets from wild-type (WT, white bars) or caveolin-1 null (Cav1-KO, black bars) mice. Data are presented as means ± SEM, n = 5. * indicates a significant difference by paired Student's t-test, P < 0.05.

lin-1 or after caveolin-1 rescue by adenovirus gene transfer. Caveolin-1-deficient fibroblasts were obtained from a patient with a recently described null mutation in the caveolin-1 gene (13). We used a Cav1-GFP adenovirus previously shown to fully substitute caveolin-1 functions (36) to monitor intracellular caveolin-1 distribution in living cells. When placed under conditions of lipid overload, all cells developed lipid droplets, visualized by Nile red staining (**Fig. 7A**), indicating that caveolin-1 is neither required for lipid droplet formation nor fatty acid uptake. Among lipid droplets found in rescued fibroblasts, some were coated with caveolin-1 but others were not (Fig. 7A). Thus, this experimental setting allowed us to determine lipid droplet size distributions on a per cell basis and to compare the size of caveolin-positive versus caveolin-negative lipid droplets. The mean size of caveolin-1 negative lipid droplets found either in caveolin-negative cells or caveolin-rescued cells was the same (Fig. 7B). This indicated that caveolin rescue per se, which is likely to restore membrane caveolae-related events (such as fatty acid uptake) had no effect
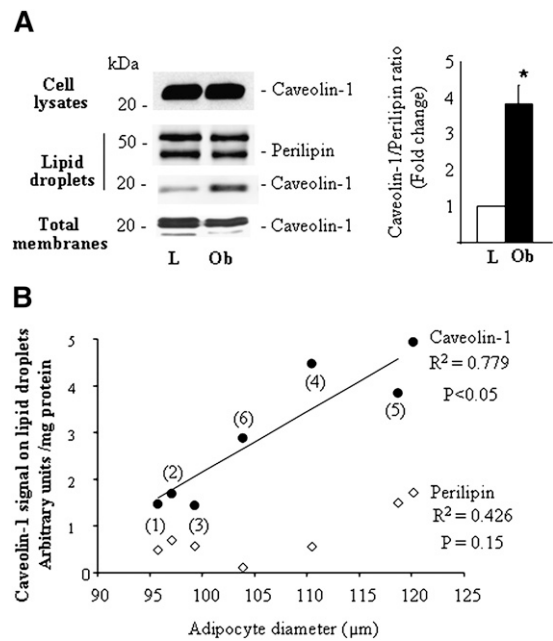

Fig. 6. Caveolin-1 specific abundance in lipid droplets is modulated in obesity and correlates with fat cell size. A: Isolated adipocytes from 16-week-old lean (L) and obese (Ob) Zucker rats were used as whole cell lysates or fractionated to prepare lipid droplets or total membranes (pooled fractions 4 to 7 as in Fig. 1B). Samples were immunoblotted with perilipin and caveolin-1 antibodies. Bars represent the ratio of caveolin to perilipin signal on lipid droplets, obtained from densitometric scanning of blots. Signal density in controls was assigned a value of 1. Four independent preparations were analyzed in each group. The asterisks signify statistically significant changes between lean and obese Zucker rats by Student's t-test (P < 0.05). B: Isolated human adipocytes from different subjects [numbered (1) to (6), see supplementary Table II] were used for lipid droplet isolation. Isolated lipid droplets were resolved by SDS-PAGE and immunoblotted with caveolin-1 and perilipin antibodies. After densitometric scanning of the blots, lipid droplet caveolin-1 or perilipin abundances were plotted as a function of adipocyte cell sizes. The numbers in brackets stand for the number assigned to each individual subject characterized in supplementary Table II. Linear regression analysis was used to evaluate the correlation between caveolin-1 (filled symbols) or perilipin (open symbols) and fat cell size. Significant correlation was found for caveolin-1 ($R^2 = 0.779$, $P = 0.0115$) but not perilipin ($R^2 = 0.4256$, $P = 0.15$).

on the size of individual lipid droplets to which caveolin did not associate. In contrast, within a single cell context for fatty acids uptake, caveolin-coated lipid droplets were significantly larger than caveolin-1-devoid lipid droplets (Fig. 7B). In agreement, the size distribution of the total pool of caveolin-1-positive lipid droplets was shifted to the right, indicating an increased proportion of caveolin-1-positive lipid droplets in the higher diameter classes (Fig. 7C), Importantly, this experiment at the single cell level allowed us to discriminate effects of caveolin rescue due to potential membrane caveolae-related events from lipid droplet-related effects. It demonstrates that caveolin-1-coated lipid droplets can grow larger than caveolin-1-devoid lipid bodies, indicating that the lipid droplet-caveolin pool can directly promote the process of lipid droplet size expansion.
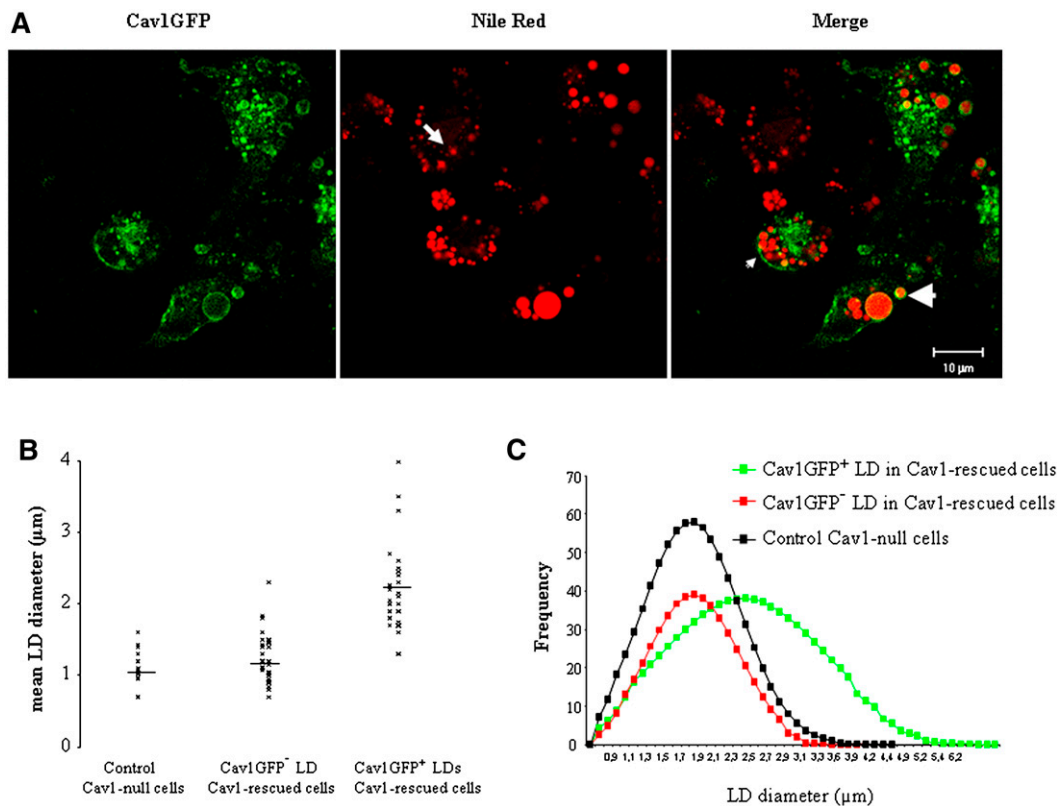
Fig. 7. Caveolin-1 coated lipid droplets (LDs) can grow larger than caveolin-1-devoid LDs. A: Confocal images of caveolin-1 deficient human fibroblasts transfected with a Cav1-GFP construct and exposed to oleic-acid (250 μM) for 2 days (medium changed daily). Cells were stained with Nile red and fixed with paraform-aldehyde prior to observation. Note that lipid droplets stained by Nile red are present in control caveolin-null cells (arrows) and in caveolin-rescued cells, as cav1GFP[+]-coated LD (large arrowhead) or cav1GFP-free LD (small arrowhead). B: Per-cell-based analysis of lipid droplet size in the presence or absence of caveolin. Lipid droplet diameters were determined from microscopy images using Image J software. The distribution of lipid droplet size within individual cells was used to determine mean LD diameter on a per cell basis. Two independent experiments were performed. Individual values corresponding to 50 cells were analyzed by ANOVA. The size of LDs with a Cav1GFP+ coat (2.01 ± 0.75 μm) was significantly higher ($P < 0.05$) than that of Cav1GFP-free LDs (1.19 ± 0.39) or LDs in control Cav1-null cells (1.11 ± 0.24). C: Diameters of individual LDs (1037) were used to establish size distributions of LD in Control Cav1-null cells (black) or in Caveolin-1-rescued cells without (Cav1GFPLD in Cav1-rescued cells (red) or with (Cav1GFP[+] LD in Cav1-rescued cells (green) a caveolin-1 coat.

DISCUSSION

It is now well recognized that caveolins can be found on lipid droplets, but the functional significance of this association remains poorly understood. This study provides the first detailed characterization of the impact of caveolins on molecular composition (both proteins and lipids) of lipid droplets, and reveals several features of the adipocyte lipid droplet caveolin pool indicative of a role in facilitating size enlargement in response to lipid filling.

First, this study identifies changes in protein and lipid composition that are likely to profoundly alter the structural organization of the lipid droplet surface. We show here that some proteins require caveolin-1 expression for lipid droplet association. The fact that several of these proteins are also found in caveolae is likely related to the plasmalemnal origin of the lipid droplet caveolin pool. Indeed, targeting of caveolin-1 to adipocyte lipid droplets involves caveolae internalization and can be blocked by inhibitors of

the endocytic pathway (19). In agreement, a recent report indicates that a member of the PTRF family, SRBC/cavin3, and caveolin-1 traffic together during caveolae vesicle internalization (37). Some caveolin-dependent lipid droplet proteins identified in the present study have membrane remodeling activity. PTRF plays a structural role in invaginated caveolae formation (29, 30) and EHD2 facilitates membrane rearrangement during fusion/fission events (38). This suggests that caveolin and associated proteins might contribute to surface remodelling on lipid droplets. This is further supported by the presence of specific alterations in caveolin-1-deficient lipid droplet phospholipids that form a shell around the neutral lipid core. Most impressive changes involved PS and lysophospholipids, found with a reduced relative abundance. Because PS is an anionic phospholipid involved in interfacial protein binding to membranes, and because some of the proteins absent in caveolin-1-deficient lipid droplets, including PTRF, annexin A1, or caveolin itself, are known to interact with PS

(29, 39, 40), it is not possible from our data to discriminate between lipids or proteins as primary causes of changes in lipid droplet composition upon caveolin deficiency. Nevertheless, reduced PS abundance on lipid droplets as well as caveolin absence is likely to modify the lipid droplet-cytoplasmic interface and consequently disturb interactions between lipid droplets and cellular components.

This study also provides a new link between caveolin lipid droplet pool and lipid droplet size. We found that adipocyte total caveolin protein concentrations were not affected by obesity in rodent models or humans, a finding that may appear contradictory to previous reports on higher caveolin mRNA expression in adipose tissues of obese rodents (41). Here, we used isolated adipocytes, and it is likely that a contribution from endothelial cells (which express caveolin-1 at the highest level) in overdeveloped obese adipose tissue but not in isolated adipocytes might account for difference with previous reports. Rather than total caveolin expression, we show that the adipocyte lipid droplet caveolin pool is profoundly affected by obesity and we point out a positive correlation with lipid droplet size. Importantly, caveolins are shown here to be differentially regulated relative to perilipin, the most abundant lipid droplet coating protein, whose relative concentration at the lipid droplet surface does not change with increasing lipid storage. Finally, a direct demonstration of the facilitation of lipid droplet expansion by caveolin-1 is provided here by the in vivo observation that within the same cellular context, individual lipid droplets coated with caveolin-1 can reach a larger size than caveolin-devoid ones.

Thus, we propose that the function of the lipid droplet caveolin pool might be to assist lipid droplet size expansion through protein-protein interaction and phospholipid remodeling of the organelle surface. Such a role for adipocyte lipid droplet caveolins might be reminiscent of their implication in mechano-transduction and shear stress response in endothelial cells (42, 43). As long as filling of the neutral lipid core of lipid droplets induces stretching of lipid droplet surface, caveolin presence might be viewed as an adaptive response to mechanical events.

The importance of surface polar lipids in lipid droplet biology recently emerged from large scale genomic screens designed to identify gene clusters involved in lipid regulation. In particular, a subset of genes linked to phospholipid synthesis was identified to control lipid droplet dynamics in *Drosophila* (44). Furthermore, the yeast homolog of the human seipin gene, which is a major cause of Berardinelli Seip congenital lipodystrophy (45), was shown to control lipid droplet size and morphology, likely through effects on surface phospholipid composition (46, 47). Our study provides a new link between caveolin and lipid droplet size enlargement, and indicates that caveolin-1 has now to be considered, like seipin and some phospholipid synthetic genes, as an important regulatory component of the lipid droplet surface organization. In agreement, gene invalidation of both seipin and caveolin-1 induces the same Berardinelli-Seip congenital lipodystrophic syndrome in humans (13).

A potential outcome of our observations relates to the study of metabolic diseases such as obesity and type 2 diabetes in which lipid overloading is a major causative factor. Emerging from rodent models, a well-accepted view is that favoring lipid storage into well-adapted specialized adipocytes can reduce lipotoxicity by limiting the spilling over of fatty acids toward other tissues (48). In this regard, caveolin-1 propensity to promote adipocyte lipid droplet expandability might be an interesting property in the search for new strategies to fight metabolic syndrome.

REFERENCES

1. Tauchi-Sato, K., S. Ozeki, T. Houjou, R. Taguchi, and T. Fujimoto. 2002. The surface of lipid droplets is a phospholipid monolayer with a unique fatty acid composition. *J. Biol. Chem.* **277:** 44507–44512.
2. Londos, C., D. L. Brasaemle, C. J. Schultz, J. P. Segrest, and A. R. Kimmel. 1999. Perilipins, ADRP, and other proteins that associate with intracellular neutral lipid droplets in animal cells. *Semin. Cell Dev. Biol.* **10:** 51–58.
3. Aboulaich, N., J. P. Vainonen, P. Stralfors, and A. V. Vener. 2004. Vectorial proteomics reveal targeting, phosphorylation and specific fragmentation of polymerase I and transcript release factor (PTRF) at the surface of caveolae in human adipocytes. *Biochem. J.* **383:** 237–248.
4. Brasaemle, D. L., G. Dolios, L. Shapiro, and R. Wang. 2004. Proteomic analysis of proteins associated with lipid droplets of basal and lipolytically stimulated 3T3–L1 adipocytes. *J. Biol. Chem.* **279:** 46835–46842.
5. Cermelli, S., Y. Guo, S. P. Gross, and M. A. Welte. 2006. The lipid-droplet proteome reveals that droplets are a protein-storage depot. *Curr. Biol.* **16:** 1783–1795.
6. Liu, P., Y. Ying, Y. Zhao, D. I. Mundy, M. Zhu, and R. G. Anderson. 2004. Chinese hamster ovary K2 cell lipid droplets appear to be metabolic organelles involved in membrane traffic. *J. Biol. Chem.* **279:** 3787–3792.
7. Wan, H. C., R. C. Melo, Z. Jin, A. M. Dvorak, and P. F. Weller. 2007. Roles and origins of leukocyte lipid bodies: proteomic and ultrastructural studies. *FASEB J.* **21:** 167–178.
8. Bartz, R., J. K. Zehmer, M. Zhu, Y. Chen, G. Serrero, Y. Zhao, and P. Liu. 2007. Dynamic activity of lipid droplets: protein phosphorylation and GTP-mediated protein translocation. *J. Proteome Res.* **6:** 3256–3265.
9. Rothberg, K. G., J. E. Heuser, W. C. Donzell, Y. S. Ying, J. R. Glenney, and R. G. Anderson. 1992. Caveolin, a protein component of caveolae membrane coats. *Cell.* **68:** 673–682.
10. Yamamoto, M., Y. Toya, C. Schwencke, M. P. Lisanti, M. G. J. Myers, and Y. Ishikawa. 1998. Caveolin is an activator of insulin receptor signaling. *J. Biol. Chem.* **273:** 26962–26968.
11. Ring, A., S. Le Lay, J. Pohl, P. Verkade, and W. Stremmel. 2006. Caveolin-1 is required for fatty acid translocase (FAT/CD36) localization and function at the plasma membrane of mouse embryonic fibroblasts. *Biochim. Biophys. Acta.* **1761:** 416–423.
12. Razani, B., T. P. Combs, X. B. Wang, P. G. Frank, D. S. Park, R. G. Russell, M. Li, B. Tang, L. A. Jelicks, P. E. Scherer, et al. 2002. Caveolin-1-deficient mice are lean, resistant to diet-induced obesity, and show hypertriglyceridemia with adipocyte abnormalities. *J. Biol. Chem.* **277:** 8635–8647.
13. Kim, C. A., M. Delepine, E. Boutet, M. H. El, L. S. Le, M. Meier, M. Nemani, E. Bridel, C. C. Leite, D. R. Bertola, et al. 2008. Association of a homozygous nonsense caveolin-1 mutation with Berardinelli-Seip congenital lipodystrophy. *J. Clin. Endocrinol. Metab.* **93:** 1129–1134.

14. Blouin, C. M., L. S. Le, F. Lasnier, I. Dugail, and E. Hajduch. 2008. Regulated association of caveolins to lipid droplets during differentiation of 3T3–L1 adipocytes. *Biochem. Biophys. Res. Commun.* **376:** 331–335.

15. Fujimoto, T., H. Kogo, K. Ishiguro, K. Tauchi, and R. Nomura. 2001. Caveolin-2 is targeted to lipid droplets, a new "membrane domain" in the cell. *J. Cell Biol.* **152:** 1079–1085.

16. Ostermeyer, A. G., J. M. Paci, Y. Zeng, D. M. Lublin, S. Munro, and D. A. Brown. 2001. Accumulation of caveolin in the endoplasmic reticulum redirects the protein to lipid storage droplets. *J. Cell Biol.* **152:** 1071–1078.

17. Pol, A., R. Luetterforst, M. Lindsay, S. Heino, E. Ikonen, and R. G. Parton. 2001. A caveolin dominant negative mutant associates with lipid bodies and induces intracellular cholesterol imbalance. *J. Cell Biol.* **152:** 1057–1070.

18. Robenek, M. J., N. J. Severs, K. Schlattmann, G. Plenz, K. P. Zimmer, D. Troyer, and H. Robenek. 2004. Lipids partition caveolin-1 from ER membranes into lipid droplets: updating the model of lipid droplet biogenesis. *FASEB J.* **18:** 866–868.

19. Le Lay, S., E. Hajduch, M. R. Lindsay, X. Le Liepvre, C. Thiele, P. Ferré, R. G. Parton, T. Kurzchalia, K. Simons, and I. Dugail. 2006. Cholesterol-induced caveolin targeting to lipid droplets in adipocytes; a role for caveolar endocytosis. *Traffic.* **7:** 549–561.

20. Cohen, A. W., T. P. Combs, P. E. Scherer, and M. P. Lisanti. 2003. Role of caveolin and caveolae in insulin signaling and diabetes. *Am. J. Physiol. Endocrinol. Metab.* **285:** E1151–E1160.

21. Briquet-Laugier V., I. Dugail, B. Ardouin, X. Le Liepvre, M. Lavau, and A. Quignard-Boulange. 1994. Evidence for a sustained genetic effect on fat storage capacity in cultured adipose cells from Zucker rats. *Am. J. Physiol.* **267:** E439–E446.

22. Rodbell, M. 1964. Metabolism of isolated fat cells- I: effects of hormones on glucose metabolism and lipolysis. *J. Biol. Chem.* **239:** 375–380.

23. Hajduch, E., D. R. Alessi, B. A. Hemmings, and H. S. Hundal. 1998. Constitutive activation of protein kinase B alpha by membrane targeting promotes glucose and system A amino acid transport, protein synthesis, and inactivation of glycogen synthase kinase 3 in L6 muscle cells. *Diabetes.* **47:** 1006–1013.

24. Mastick, C. C., and A. R. Saltiel. 1997. Insulin-stimulated tyrosine phosphorylation of caveolin is specific for the differentiated adipocyte phenotype in 3T3–L1 cells. *J. Biol. Chem.* **272:** 20706–20714.

25. Shevchenko, A., M. Wilm, O. Vorm, and M. Mann. 1996. Mass spectrometric sequencing of proteins silver-stained polyacrylamide gels. *Anal. Chem.* **68:** 850–858.

26. Perkins, D. N., D. J. Pappin, D. M. Creasy, and J. S. Cottrell. 1999. Probability-based protein identification by searching sequence databases using mass spectrometry data. *Electrophoresis.* **20:** 3551–3567.

27. Rolland, V., X. Le Liepvre, D. B. Jump, M. Lavau, and I. Dugail. 1996. A GC-rich region containing Sp1 and Sp1-like binding sites is a crucial regulatory motif for Fatty Acid Synthase Gene promoter activity in adipocytes. *J. Biol. Chem.* **271:** 21297–21302.

28. Bligh, E. G., and W. J. Dyer. 1959. A rapid method of total lipid extraction and purification. *Can. J. Biochem. Physiol.* **37:** 911–917.

29. Hill, M. M., M. Bastiani, R. Luetterforst, M. Kirkham, A. Kirkham, S. J. Nixon, P. Walser, D. Abankwa, V. M. Oorschot, S. Martin, et al. 2008. PTRF-Cavin, a conserved cytoplasmic protein required for caveola formation and function. *Cell.* **132:** 113–124.

30. Liu, L., and P. F. Pilch. 2008. A critical role of cavin (polymerase I and transcript release factor) in caveolae formation and organization. *J. Biol. Chem.* **283:** 4314–4322.

31. Izumi, T., Y. Shibata, and T. Yamamoto. 1988. Striped structures on the cytoplasmic surface membranes of the endothelial vesicles of the rat aorta revealed by quick-freeze, deep-etching replicas. *Anat. Rec.* **220:** 225–232.

32. Monier, S., R. G. Parton, F. Vogel, J. Behlke, A. Henske, and T. V. Kurzchalia. 1995. VIP21-caveolin, a membrane protein constituent of the caveolar coat, oligomerizes in vivo and in vitro. *Mol. Biol. Cell.* **6:** 911–927.

33. Thomsen, P., K. Roepstorff, M. Stahlhut, and B. van Deurs. 2002. Caveolae are highly immobile plasma membrane microdomains, which are not involved in constitutive endocytic trafficking. *Mol. Biol. Cell.* **13:** 238–250.

34. Pol, A., S. Martin, M. A. Fernandez, M. Ingelmo-Torres, C. Ferguson, C. Enrich, and R. G. Parton. 2005. Cholesterol and fatty acids regulate dynamic caveolin trafficking through the Golgi complex and between the cell surface and lipid bodies. *Mol. Biol. Cell.* **16:** 2091–2105.

35. Bray, G. A., and D. A. York. 1979. Hypothalamic and genetic obesity in experimental animals: an autonomic and endocrine hypothesis. *Physiol. Rev.* **59:** 719–809.

36. Pelkmans, L., J. Kartenbeck, and A. Helenius. 2001. Caveolar endocytosis of simian virus 40 reveals a new two-step vesicular-transport pathway to the ER. *Nat. Cell Biol.* **3:** 473–483.

37. McMahon, K. A., H. Zajicek, W. P. Li, M. J. Peyton, J. D. Minna, V. J. Hernandez, K. Luby-Phelps, and R. G. Anderson. 2009. SRBC/cavin-3 is a caveolin adapter protein that regulates caveolae function. *EMBO J.* **28:** 1001–1015.

38. Daumke, O., R. Lundmark, Y. Vallis, S. Martens, P. J. Butler, and H. T. McMahon. 2007. Architectural and mechanistic insights into an EHD ATPase involved in membrane remodelling. *Nature.* **449:** 923–927.

39. Le Lan, C., J. M. Neumann, and N. Jamin. 2006. Role of the membrane interface on the conformation of the caveolin scaffolding domain: a CD and NMR study. *FEBS Lett.* **580:** 5301–5305.

40. Patel, D. R., J. M. Isas, A. S. Ladokhin, C. C. Jao, Y. E. Kim, T. Kirsch, R. Langen, and H. T. Haigler. 2005. The conserved core domains of annexins A1, A2, A5, and B12 can be divided into two groups with different Ca2+-dependent membrane-binding properties. *Biochemistry.* **44:** 2833–2844.

41. Soukas, A., P. Cohen, N. D. Socci, and J. M. Friedman. 2000. Leptin-specific patterns of gene expression in white adipose tissue. *Genes Dev.* **14:** 963–980.

42. Yu, J., S. Bergaya, T. Murata, I. F. Alp, M. P. Bauer, M. I. Lin, M. Drab, T. V. Kurzchalia, R. V. Stan, and W. C. Sessa. 2006. Direct evidence for the role of caveolin-1 and caveolae in mechanotransduction and remodeling of blood vessels. *J. Clin. Invest.* **116:** 1284–1291.

43. Frank, P. G., and M. P. Lisanti. 2006. Role of caveolin-1 in the regulation of the vascular shear stress response. *J. Clin. Invest.* **116:** 1222–1225.

44. Guo, Y., C. Walther, M. Rao, N. Stuurman, G. Goshima, K. Terayama, J. S. Wong, R. D. Vale, P. Walter, and R. V. Farese. 2008. Functional genomic screen reveals genes involved in lipid-droplet formation and utilization. *Nature.* **29:** 657–661.

45. Magre, J., M. Delepine, E. Khallouf, T. Gedde-Dahl, Jr., M. L. Van, E. Sobel, J. Papp, M. Meier, A. Megarbane, A. Bachy, et al. 2001. Identification of the gene altered in Berardinelli-Seip congenital lipodystrophy on chromosome 11q13. *Nat. Genet.* **28:** 365–370.

46. Szymanski, K. M., D. Binns, R. Bartz, N. V. Grishin, W. P. Li, A. K. Agarwal, A. Garg, R. G. Anderson, and J. M. Goodman. 2007. The lipodystrophy protein seipin is found at endoplasmic reticulum lipid droplet junctions and is important for droplet morphology. *Proc. Natl. Acad. Sci. USA.* **104:** 20890–20895.

47. Fei, W., G. Shui, B. Gaeta, X. Du, L. Kuerschner, P. Li, A. J. Brown, M. R. Wenk, R. G. Parton, and H. Yang. 2008. Fld1p, a functional homologue of human seipin, regulates the size of lipid droplets in yeast. *J. Cell Biol.* **180:** 473–482.

48. Le Lay, S., and I. Dugail. 2009. Connecting lipid droplet biology and the metabolic syndrome. *Prog. Lipid Res.* **48:** 191–195.